Effects of Somatostatin Analogues on Retinal Angiogenesis in a Mouse Model of Oxygen-Induced Retinopathy: Involvement of the Somatostatin Receptor Subtype 2

Massimo Dal Monte, Chiara Ristori, Maurizio Cammalleri, and Paola Bagnoli

Purpose. To determine whether selective activation or blockade of the somatostatin (SRIF) receptor 2 (sst_2) with two SRIF analogues, octreotide and D-Tyr^8 cyanamid 154806 (CYN), influences retinal vascularization and levels of vascular endothelial growth factor (VEGF) and its receptors VEGFR-1 and -2 in a mouse model of oxygen-induced retinopathy (OIR).

Methods. Wild-type (WT), sst_1-knockout (KO), and sst_2-KO mice were used. The OIR model was used to test the effects of octreotide and CYN administered subcutaneously. Retinopathy was assessed by a retinal scoring system using fluorescein-perfused retinal wholemounts. Retinal levels of VEGF, VEGFR-1, and -2 were evaluated with quantitative RT-PCR, Western blot, and ELISA.

Results. In both WT and sst_1-KO mice, OIR-induced neovascularization was reduced by octreotide, whereas it was increased by CYN. No effects of octreotide and CYN on retinal neovascularization were observed in sst_2-KO retinas. Hypoxia upregulated the expression of VEGF and its receptors. Compared with WT retinas, the increase in VEGF, but not in VEGF receptors, was less pronounced in sst_1-KO retinas in which sst_2 is known to be overexpressed. The hypoxia-induced increase in VEGF and its receptors was affected by SRIF analogues, with ameliorative effects of octreotide and worsening effects of CYN, which were more pronounced in the presence of sst_2 overexpression.

Conclusions. These data suggest that sst_2 regulates angiogenic responses to the hypoxic insult through a modulation of retinal levels of VEGF and its receptors. The present results further support the possibility of the use of sst_2-selective ligands in the treatment of retinopathy. (*Invest Ophthalmol Vis Sci.* 2009;50: 3596–3606) DOI:10.1167/iovs.09-3412

Neovascular ocular diseases represent a major health threat to all age groups and especially the rapidly increasing diabetic patient population. Proliferative diabetic retinopathy is the leading cause of blindness in the young-to-middle-age population in the Western world. Although the vascular insult varies across different neovascular ocular diseases, the proliferation of aberrant blood vessels is common to all.

The naturally occurring growth hormone inhibitor, somatostatin (somatotropin release-inhibiting factor, SRIF) and its receptors (sst_1–sst_5)[1] are found in the neuroretina of humans and other mammals, and growing evidence suggests that in the retina, SRIF acts both as a neuromodulator and an antiangiogenic factor (for a review, see Ref. 2). In particular, there is a general agreement that SRIF combats neovascularization associated with diabetic retinopathy,[3] although the mechanism of action remains to be elucidated.

There is evidence mostly from in vitro studies that sst_2 may mediate the angioinhibitory activity of SRIF.[4] However, little is known of the effects of sst_2 activation on neovascularization and its associated factors in in vivo models. Ameliorating effects of the sst_2-preferring agonist octreotide on neovascularization with concomitant reduction of the levels of vascular endothelial growth factor (VEGF) have been recently demonstrated in rat models of portal hypertension.[5,6] In recent years, octreotide has been used in clinical trials of diabetic retinopathy treatments, but with conflicting results.[7,8] In a mouse model of oxygen-induced retinopathy (OIR), there is indication that sst_2 agonists, including octreotide, inhibit retinal neovascularization.[9–11] In this model, we have recently demonstrated that the severity of angiogenic responses to hypoxia is correlated to the expression level of sst_2 in the retina.[12] The lack of sst_2, as in sst_2-knockout (KO) retinas, is associated with the more severe effects of hypoxia on retinal neovascularization and proangiogenic factors, whereas a chronic overexpression of sst_2 (consequent to the genetic deletion of sst_1 as in sst_1-KO retinas[13,14]) attenuates hypoxia's effects on proangiogenic factors. Thus, the use of these KO mice represents a useful tool for assessing the effect of SRIF analogues on hypoxia-induced retinal neovascularization. In the present study, retinas of wild-type (WT) and sst_1- and sst_2-KO mice were rendered hypoxic and were used to investigate whether sst_2 activation or blockade influences vascular responses to the hypoxic insult and its associated factors. sst_2-KO mice were used as a control to assess the specific action of SRIF analogues on sst_2. Since the severity of angiogenic responses to hypoxia appears to be related to the expression level of sst_2, in sst_1-KO mice we evaluated whether sst_2 overexpression influences octreotide's or CYN's effects on angiogenic responses to the hypoxic insult.

Materials and Methods

Octreotide was purchased from NeoMPS (Strasbourg, France). The PCR mastermix (iQ Sybr Green Supermix) was from Bio-Rad (Hercules, CA). Primers were obtained from MWG Biotech (Ebersberg, Germany). A nucleic acid gel stain (GelStar) was obtained from Cambrex (East Rutherford, NJ). Rabbit polyclonal antibodies to VEGF, VEGFR-1, and VEGFR-2 were obtained from Santa Cruz Biotechnologies (Santa Cruz, CA). Enhanced chemiluminescence reagent was from Millipore (Billerica, MA). All other chemicals were obtained from Sigma-Aldrich (St. Louis, MO).

Animals

Experiments were performed on 265 mice of WT (C57BL/6) and sst_1- or sst_2-KO strains of both sexes at postnatal day (PD) 17 (6 g body weight). sst_1- and sst_2-KO mice were generated as previously reported.[15,16] Experiments were performed in accordance with the ARVO Statement

From the Dipartimento di Biologia, Università di Pisa, Pisa, Italy.

Supported by the Italian Ministry of University and Research (MUR, PRIN, Grant 2005052312).

Submitted for publication January 15, 2009; revised March 3, 2009; accepted June 5, 2009.

Disclosure: **M. Dal Monte**, None; **C. Ristori**, None; **M. Cammalleri**, None; **P. Bagnoli**, None

The publication costs of this article were defrayed in part by page charge payment. This article must therefore be marked "*advertisement*" in accordance with 18 U.S.C. §1734 solely to indicate this fact.

Corresponding author: Paola Bagnoli, Dipartimento di Biologia, Università di Pisa, Via San Zeno, 31-56127 Pisa, Italy; pbagnoli@biologia.unipi.it.

Investigative Ophthalmology & Visual Science, August 2009, Vol. 50, No. 8

for the Use of Animals in Ophthalmic and Vision Research and in compliance with the Italian law on animal care No. 116/1992 and the EEC/609/86. All efforts were made to reduce the number of animals used.

Model of Hypoxia-Induced Retinopathy

In a typical model of hypoxia-induced retinopathy,[17] litters of mouse pups with their nursing mothers were exposed in an infant incubator to high oxygen concentration (75% ± 2%) between PD7 and PD12, before return to room air between PD12 and PD17. Oxygen was checked twice daily with an oxygen analyzer (Miniox I; Bertocchi srl Elettromedicali, Cremona, Italy). Individual litters were reared in either oxygen or room air. Within litters, differential treatment was performed including no treatment, octreotide, CYN, and sham injection. The animals were treated with injections for 5 days from PD12 to PD16. They were anesthetized by ip injection of Avertin (1.2% tribromoethanol and 2.4% amylene hydrate in distilled water; 0.02 mL/g body weight). All experiments were performed at the same time of day to exclude possible circadian influences. The data were collected from both males and females and the results combined, as there was no apparent sex difference.

Administration of SRIF Analogues

The sst_2-preferring peptidyl agonist octreotide and the sst_2-selective peptidyl antagonist D-Tyr^8 cyanamid 154806 (CYN)[18,19] were given twice daily subcutaneously from PD12 to PD16. Octreotide was used at 0.02 mg kg^{-1} $dose^{-1}$.[10,11] CYN was used at concentrations ranging from 0.01 to 2.0 mg kg^{-1} $dose^{-1}$ in agreement with previous works using sst_2 antagonists.[20–24] Comparable concentrations of nonpeptide SRIF receptor agonists were recently used by Palii et al.[9] in the OIR model. In rats, the SRIF analogue BIM-23627 has been found to exert antagonistic effects on sst_2 after subcutaneous administration.[21] The analogues were dissolved in 33 mM acetate buffer (pH 5) with 135 mM NaCl. Sham injections were performed with that vehicle.

Assessment of Retinal Vascularization

Fluorescein-conjugated dextran perfusion of the retinal vessels was performed as previously described.[25] Briefly, in anesthetized animals a median sternotomy was performed, and the left ventricle was perfused with 2 mL of a 25-mg/mL solution of fluorescein-conjugated dextran in 0.15 M phosphate buffer. The eyes were enucleated, the retinas were dissected, and flatmounts were obtained. They were viewed by fluorescence microscopy (Eclipse E800; Nikon, Badhoevedorp, Netherlands), and images were acquired (DFC320 camera; Leica Microsystems, Wetzlar, Germany). Neovascularization was evaluated by using the retinopathy scoring system shown in Table 1 according to previously published protocols.[11] Three trained observers evaluated the number of clock hours with abnormal vessels for each retina. The data were averaged and are expressed in values ranging from 0 to 11.

Isolation of Retinal RNA and cDNA Preparation

After death, the eyes were rapidly removed and retinas were dissected, immediately frozen in liquid nitrogen, and stored at −80°C. Total RNA from four samples (each containing three retinas) for each experimental condition was extracted (RNeasy Mini Kit; Qiagen, Valencia, CA), according to the manufacturer's instructions. The purified RNA was suspended in RNase-free water and quantified spectrophotometrically (SmartSpec 3000; Bio-Rad). First-strand cDNA was generated from 1 μg of total RNA (QuantiTect Reverse Transcription Kit; Qiagen). cDNA samples were aliquoted and stored at −20°C.

Real-Time Quantitative RT-PCR

Real-time quantitative RT-PCR (QPCR) was performed with a kit (SYBR Green on MiniOpticon Two-Color Real-time PCR detection system; Bio-Rad). QPCR primer sets were designed with Primer3 software[26] (VEGFR-1 and -2) or obtained from either Primer Bank[27] (VEGF) or RTPrimerDB[28] (Rpl13a). Forward and reverse primers were chosen to hybridize to unique regions of the appropriate gene sequence; their sequences are listed in Table 2. PCR reactions including 1 μL of cDNA, 300 nM of each primer, 7.5 μL of mastermix (iQ Sybr Green Supermix; Bio-Rad), and RNase-free water to complete the reaction mixture volume to 15 μL. Each target gene was run concurrently with Rpl13a, a constitutively expressed control gene. Negative control reactions were set up as just described, but without any template cDNA. All reactions were run in triplicate. The QPCR was performed with hot-start denaturation step at 95°C for 3 minutes, and then was performed for 40 cycles at 95°C for 10 seconds and 58°C for 20 seconds. The fluorescence was read during the reaction, allowing a continuous monitoring of the amount of PCR product. Primers were initially used to generate a standard curve over a large dynamic range of starting cDNA quantity which allows calculation of the amplification efficiency for each of the primer pairs (Table 2). After amplification, first derivative melting curve analysis was used to confirm that the signal corresponded to a unique amplicon. QPCR products were analyzed by nucleic acid staining on a gel stain (GelStar; Cambrex) containing 3% agarose to verify the correct product size. As previously described, samples were compared by using the relative cycle threshold (CT method).[29] The increase or decrease (*x*-fold) was determined relative to a control after normalizing to RPL13a. All reactions were run in triplicate. After statistical analysis, the data from the different experiments were plotted and averaged in the same graph.

Western Blot Analysis

Western blot analysis was performed on proteins extracted from three samples for each experimental condition, as previously described.[14] Each sample contained five retinas. Briefly, retinas were homogenized in 10 mM Tris-HCl (pH 7.6) containing 5 mM EDTA, 3 mM EGTA, 250 mM sucrose, 1 mM phenylmethylsulfonyl fluoride, 1 μM pepstatin, 10 μg/mL leupeptin, and 2 μg/mL aprotinin (buffer A) and centrifuged at 22,000*g* for 30 minutes at 4°C. The supernatant was used for VEGF detection. The pellet was resuspended in 20 mM HEPES (pH 7.4)

Table 1. Retinopathy Scoring System

	Points				
Criteria	**0**	**1**	**2**	**3**	**4**
Blood vessel tufts	None	In <3 clock hours	In 3–5 clock hours	In 6–8 clock hours	In 9–12 clock hours
Central vasoconstriction	None	Mild, early zone 1 (inner 50% of zone 1)	Moderate, throughout zone 1 (outer 50% of zone 1)	Severe, extending to zone 2	
Retinal hemorrhage	Absent	Present			
Blood vessel tortuosity	None	<1/3 of vessels	1/3–2/3 of vessels	>2/3 of vessels	

Flatmounted retinas were examined by fluorescence microscopy, and retinopathy was quantified according to four criteria. Points received for each criterion were summed to obtain the retinopathy score. A higher score (range 0–11) indicates more severe retinopathy. The scoring system was adapted from Higgins et al.[11]

TABLE 2. Primers for PCR Analysis

Gene	Primer Sequence	Product Length (bp)	QPCR: Amplification Efficiency* (%)	Gene Bank Accession No.
VEGF	Forward: GCACATAGGAGAGATGAGCTTCC Reverse: CTCCGCTCTGAACAAGGCT	105	98.8	NM_009505
VEGFR-1	Forward: GAGGAGGATGAGGGTGTCTATAGGT Reverse: GTGATCAGCTCCAGGTTTGACTT	116	95.5	NM_010228
VEGFR-2	Forward: GCCCTGC TGTGGTCTCACTAC Reverse: CAAAGCATTGCCCATTCGAT	114	96.4	NM_010612
Rpl13a	Forward: CACTCTGGAGGAGAAACGGAAGG Reverse: GCAGGCATGAGGCAAACAGTC	182	97.3	NM_009438

* Data calculated by Opticon Monitor 3 software (Bio-Rad).

containing 150 mM NaCl, 5 mM EDTA, 3 mM EGTA, 4 mg/mL *n*-dodecyl-β-maltoside, and the proteinase inhibitors just listed and centrifuged at 22,000*g* for 30 minutes at 4°C. The supernatant was used to detect either VEGFR-1 or -2. Protein concentration was determined according to Bradford,[30] with bovine serum albumin used as a standard. Aliquots of each sample containing equal amounts of protein were subjected to 10% sodium dodecyl sulfate–polyacrylamide gel electrophoresis according to Laemmli.[31] β-Actin was used as the loading control. The gels were transblotted onto polyvinylidene difluoride membrane, and the blots were blocked for 1 hour at room temperature with 3% milk. The blots were then incubated overnight at 4°C with primary rabbit polyclonal antibodies directed to VEGF (1:200 dilution), VEGFR-1 (1:100 dilution), and VEGFR-2 (1:100 dilution) or with a primary mouse monoclonal antibody directed to β-actin (1:2500 dilution). Finally, blots were incubated for 1 hour at room temperature with mouse anti-rabbit horseradish peroxidase–labeled secondary antibody (1:5000 dilution) or with rabbit anti-mouse horseradish peroxidase-labeled secondary antibody (1:25,000 dilution) and developed with the enhanced chemiluminescence reagent. The optical density (OD) of the bands was evaluated on computer (Quantity One software; Bio-Rad). The data were normalized to the level of β-actin. All experiments were run in duplicate. After statistical analysis, data from the different experiments were plotted and averaged in the same graph.

Enzyme-Linked Immunosorbent Assay

VEGF protein concentration was determined on retinal lysate by enzyme-linked immunosorbent assay (ELISA) according to the manufacturer's protocol (Quantikine Mouse VEGF ELISA kit; R&D Systems, Minneapolis, MN). The measurement was performed on three samples for each experimental condition. According to Nagai et al.,[32] two retinas for each sample were placed into 200 μL of buffer A and sonicated for 30 seconds at 50 Hz. The lysate was centrifuged at 22,000*g* for 15 minutes at 4°C. Protein concentration was measured as just described. VEGF concentration was determined spectrophotometrically (Microplate Reader 680 XR; Bio-Rad) at 450 nm. In each experiment, all samples and standards were measured in duplicate. Data were collected as picograms VEGF per milligrams of total protein and, after statistics, averaged in the same graph.

Statistical Analysis

Retinopathy scores were evaluated by the Kruskal-Wallis test for the overall group and by the Dunn's post hoc test to determine differences between groups. Retinopathy score data are represented as the median (25th, 75th quartiles). All other data were analyzed by the Kolmogorov-Smirnov test on verification of normal distribution. Statistical significance was evaluated with ANOVA followed by the Newman-Keuls multiple-comparison test. The results are expressed as mean ± SE of data for the indicated *n* values (Prism; GraphPad Software, San Diego, CA). Differences with $P < 0.05$ were considered significant.

RESULTS

Retinal Neovascularization

In agreement with Dal Monte et al.,[12] we found that hypoxic retinas of WT and sst_1-KO mice did not significantly differ in their median total retinopathy score, whereas the median retinopathy score in sst_2-KO retinas was significantly higher than in WT or sst_1-KO mice ($P < 0.01$, Table 3). Vehicle injections did not affect neovascularization in any strain. WT and sst_1-KO pups treated with octreotide had a significant improvement in their retinopathy scores when compared with oxygen and oxygen+vehicle–treated animals ($P < 0.05$, Table 3). In both WT and sst_1-KO mice, the retinopathy score was significantly increased by CYN at a dose of 0.5 mg kg^{-1} ($P < 0.01$ in WT and $P < 0.05$ in sst_1-KO, Table 3). In sst_2-KO mice treated with octreotide or CYN, the median retinopathy score did not differ from that measured in oxygen and oxygen+vehicle–treated mice. No differences were found between oxygen and oxygen+vehicle–treated mice when compared with mice treated with octreotide or with CYN with respect to the different subscores, except for the score for blood vessels tufts. In both WT and sst_1-KO mice, octreotide treatment caused a significant decrease in blood vessel tufts with respect to untreated or vehicle-treated animals. The opposite (i.e., a significant increase in blood vessel tufts) was obtained after CYN treatment. Representative retinal wholemounts of WT and KO mice are shown in Figure 1.

VEGF, VEGFR-1, and VEGFR-2

We evaluated whether selective activation or blockade of sst_2 with SRIF analogues may be related to variations in retinal levels of VEGF and its receptors, VEGFR-1 and -2, in the OIR model of WT and sst_1-KO mice. In all experiments, vehicle treatment did not affect retinal the levels of VEGF, VEGFR-1, or VEGFR-2.

Messengers

QPCR yielded amplified products at 105, 116, and 114 bp, which correspond to VEGF, VEGFR-1, and VEGFR-2 mRNA, respectively (Fig. 2A). In agreement with Dal Monte et al.,[12] our findings showed that hypoxic retinas of WT and sst_1-KO mice displayed significantly increased levels of VEGF, VEGFR-1, and VEGFR-2 mRNA. In particular, the relative increase in VEGF mRNA was lower in sst_1-KO than in WT mice, whereas that in VEGF receptor messengers did not differ significantly between WT and sst_1-KO mice (Figs. 2B–D). As shown in Figure 3, in WT, octreotide decreased significantly the hypoxia-induced increase in VEGF and VEGFR-2 messengers (~27% and 30%, respectively, $P < 0.05$), whereas it did not affect VEGFR-1 mRNA. In sst_1-KO, octreotide significantly decreased the VEGF, VEGFR-1, and VEGFR-2 messengers (~38%, 44% and 31%, re-

TABLE 3. Retinopathy Subscores and Total Score

	WT				sst_1 KO				sst_2 KO			
	Hypoxia	+ Vehicle	+ Octreotide	+ Cyanamid	Hypoxia	+ Vehicle	+ Octreotide	+ Cyanamid	Hypoxia	+ Vehicle	+ Octreotide	+ Cyanamid
Number of animals	6	6	12	8	6	6	10	8	6	6	6	6
Blood vessel tufts	2 (1, 2)	2 (1.5, 2.5)	1 (1, 2)*	3 (2, 3.5)†	2 (1, 2)	1.5 (1, 2)	1 (1, 1)*	2.5 (2, 3)*	4 (2.5, 4)‡	3.5 (2.5, 4)§	3.5 (2.5, 4)	4 (2.5, 4)
Central vasoconstriction	1 (1, 1)	1 (1, 1)	1 (1, 1)	1 (1, 2)	1 (1, 1)	1 (1, 1.5)	1 (1, 2)	1 (1, 1.5)	3 (2.5, 3)‡	3 (2, 3)§	3 (2.5, 3)	3 (2.5, 3)
Hemorrhage	1 (0, 1)	1 (0, 1)	1 (0, 1)	1 (0, 1)	1 (0, 1)	1 (0.5, 1)	1 (0, 1)	1 (0.5, 1)	1 (1, 1)	1 (1, 1)	1 (1, 1)	1 (1, 1)
Blood vessel tortuosity	2 (1, 2)	2 (1, 2)	2 (1, 2)	2 (1, 2)	2 (1, 2)	2 (1, 2)	2 (1, 2)	2 (1, 2)	3 (2, 3)‡	3 (2, 3)§	3 (2.5, 3)	3 (2, 3)
Total retinopathy score	6 (5, 6)	6 (5, 6)	5 (4, 5)*	7 (6, 8.5)†	6 (5, 6)	6 (5, 6)	5 (4, 5)*	6 (5.5, 7)*	10 (9, 11)‡	10 (8.5, 10.5)§	10 (9, 11)	10 (9, 11)

Data are expressed as the median (25th, 75th quartiles).
* $P < 0.05$ vs. respective vehicle treated.
† $P < 0.01$ vs. respective vehicle treated.
‡ $P < 0.01$ vs. hypoxic WT.
§ $P < 0.01$ vs. vehicle treated WT (Kruskal-Wallis, followed by Dunn's post hoc test).

spectively, $P < 0.05$). In both WT and sst_1-KO mice, CYN at a dose of 0.5 mg kg^{-1} increased significantly the relative levels of VEGF and VEGFR-2 messengers (in WT: ~62%, $P < 0.01$ and 47%, $P < 0.05$, respectively; in sst_1-KO: ~40% and 32%, respectively, $P < 0.05$), whereas it did not affect VEGFR-1 mRNA. In sst_1-KO mice, the CYN-induced increase in VEGF mRNA was significantly lower than that observed in WT mice (~15%, $P < 0.05$).

Proteins

To test whether the effects of octreotide or CYN on VEGF and VEGF receptor messengers would have comparable effects on VEGF and VEGF receptor proteins, mice were treated with SRIF analogues, and protein content was analyzed by Western blot and ELISA. Densitometric analysis of the immunoblots demonstrated that normoxic retinas of WT and sst_1-KO mice had comparable levels of VEGF, VEGFR-1, and VEGFR-2 and that hypoxia significantly increased these levels, in agreement with previous results (Fig. 4).[12] As shown in Figure 5A, in hypoxic mice treated with vehicle, VEGF levels were significantly lower in sst_1-KO than in WT (~15%, $P < 0.05$). As also shown in Figure 5A, octreotide significantly decreased VEGF protein expression in both WT and sst_1-KO mice (~19% and 22%, respectively, $P < 0.05$) with stronger effects in sst_1-KO than in WT (~17%, $P < 0.05$). In contrast, CYN at 0.5 mg kg^{-1} significantly increased VEGF protein in both WT and sst_1-KO (~20% and 18%, respectively, $P < 0.05$). The CYN-induced increase in VEGF was significantly lower in sst_1-KO than in WT (~16%, $P < 0.05$). The relative levels of VEGF receptors did not differ significantly between WT and sst_1-KO (Figs. 5B, 5C). Octreotide did not affect VEGFR-1 protein in the WT, but reduced its level in the sst_1-KO (~25%, $P < 0.05$). In contrast, VEGFR-2 protein was comparably reduced by octreotide in either WT or sst_1-KO (~16% and 30%, respectively, $P < 0.05$). VEGFR-1 protein was unaffected by CYN in both WT and sst_1-KO, whereas VEGFR-2 protein was comparably increased by CYN in both strains (~27% and 19%, respectively, $P < 0.05$). To confirm the data obtained with Western blot and to evaluate whether the effects of SRIF analogues in sst_1-KO mice were dependent on sst_2 overexpression, VEGF protein levels were quantitated with ELISA. In agreement with results from the Western blot analysis, normoxic VEGF was significantly increased by hypoxia in both WT and sst_1-KO retinas (Fig. 6A). The VEGF increase was lower in sst_1-KO than in WT (~28%, $P < 0.01$). Measurements of VEGF levels in normoxic retinas are in line with previous results in the rodent retina.[32–34] Our determination of VEGF levels after hypoxia gave values in the range of those previously reported in mice.[34,35] As shown in Figure 6B, ELISA quantitation confirmed a significant decrease in VEGF protein formation in octreotide-treated animals of both strains (~32% and 31%, respectively, $P < 0.05$). After octreotide, the VEGF level in sst_1-KO retinas was lower than in WT retinas (~23%, $P < 0.05$). WT mice treated with CYN at 0.5 mg kg^{-1} showed a significant increase in VEGF levels (~99%, $P < 0.001$). In sst_1-KO mice, a dose-dependent increase in VEGF was observed after treatment with increasing concentrations of CYN with no effects at 0.01 mg kg^{-1}, an increase at 0.5 mg kg^{-1} (~77%, $P < 0.01$) but significantly lower than in WT (~36%, $P < 0.01$), and reaching a maximum at 2.0 mg kg^{-1}, a concentration four times higher than that used in the WT (~150%, $P < 0.001$).

DISCUSSION

The results of this study add further evidence to the notion that sst_2 is protective against angiogenesis and indicate for the first time that antiangiogenic effects of sst_2 may be mediated by an

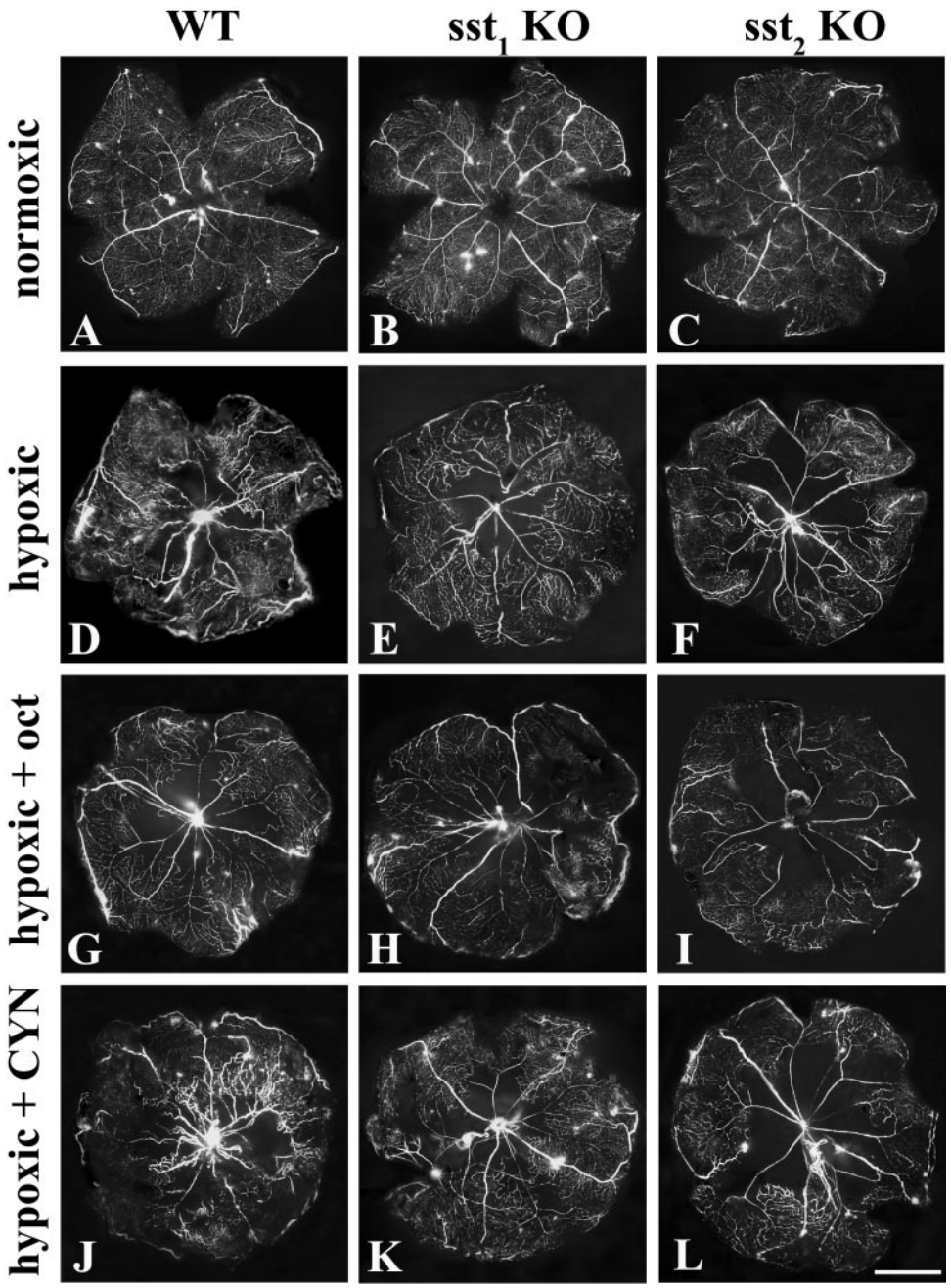

FIGURE 1. Flatmounted retinas perfused with fluorescein-dextran of PD17 WT (**A**, **D**, **G**, **J**), sst_1 (**B**, **E**, **H**, **K**)- and sst_2 (**C**, **F**, **I**, **L**)-KO mice exposed to room air (**A–C**) or to 75% ± 2% oxygen from PD7 to PD12 (**D–L**), untreated (**D–F**) or treated with SRIF analogues (octreotide in **G–I** and CYN in **J–L**). Hyperoxia followed by normoxia for 5 days produced the central loss of blood vessels and the formation of vessel tufts with more evident effects in sst_2-KO retinas. In both WT and sst_1-KO retinas, octreotide provided improvement in blood vessel tufts, whereas CYN increased pathologic retinal vascularization. SRIF analogues were without effects in sst_2-KO retinas. Scale bar, 1 mm.

sst_2-induced downregulation of the VEGF system in the OIR model.

SRIF Analogues

An ameliorating effect of octreotide on retinal neovascularization has been previously demonstrated.[9–11] In addition, in the OIR model, systemic administration of non–peptidyl SRIF receptor agonists has been shown to inhibit retinal neovascularization in a dose-dependent manner, comparable to octreotide.[9] As previously reported, octreotide may act on SRIF receptors other than sst_2 (i.e., sst_3 and sst_5), according to the affinity data in vitro, but octreotide affinity for sst_2 is higher than that for sst_3 and sst_5.[36] Although it is difficult to conjecture about the actual drug concentration that reaches the retina, we cannot exclude an involvement of sst_3 and/or sst_5 in the observed effects. On the other hand, evidence of sst_3 and sst_5 presence/localization in the retina are still elusive.[2] In addition, selective agonists for sst_3 and sst_5 have been found to elicit no effects in the mouse retina.[37] Finally, our previous finding that the lack of sst_2 is associated with heavier effects of hypoxia on retinal neovascularization[12] highlights an important role of sst_2 on retinal angiogenesis. That ameliorating effects of octreotide in the OIR model are mediated by sst_2 is demonstrated by the lack of effects in sst_2-KO mice shown in the present study.

CYN is a synthetic peptide with in vitro and in vivo properties consistent with a pure sst_2 antagonist.[18,19] CYN effects in vivo are scarcely documented. In rats, CYN administration affects the activity of mesenteric afferent fibers innervating the jejunum.[24] In the acute pilocarpine rat seizure model, the anticonvulsant effects of angiotensin IV are influenced by intracerebroventricular administration of CYN.[38] In the rat stria-

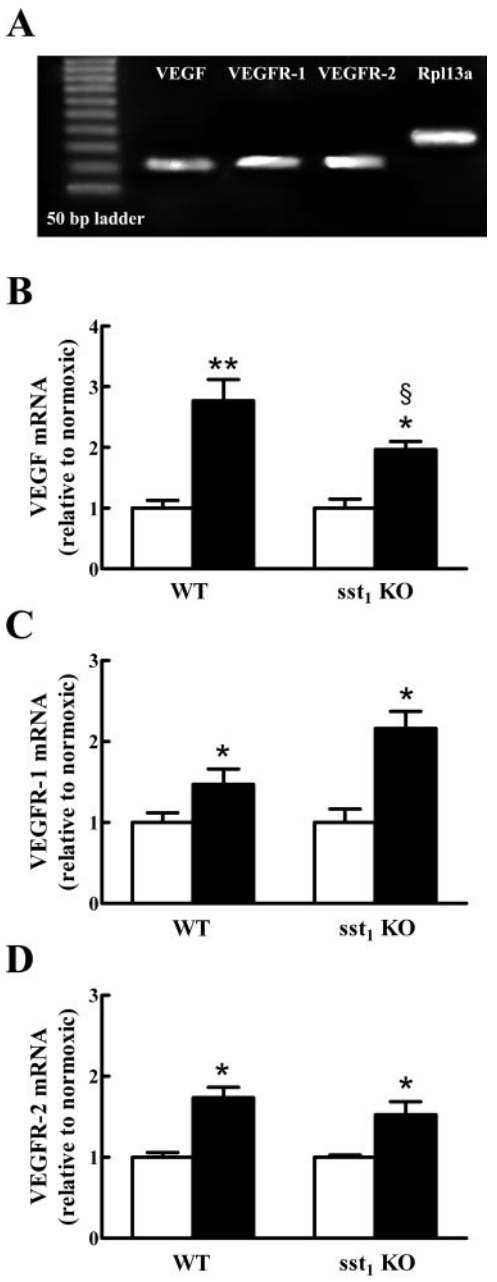

FIGURE 2. Levels of VEGF, VEGFR-1, and VEGFR-2 mRNAs in mouse retinas. (**A**) PCR products of VEGF (105 bp), VEGFR-1 (116 bp), and VEGFR-2 (114 bp) and the housekeeping gene *Rpl13a* (182 bp) in normoxic WT retinas. (**B–D**) VEGF, VEGFR-1, and VEGFR-2 mRNAs in normoxic (□) and hypoxic (■) conditions. QPCR evaluation showed that VEGF, VEGFR-1, and VEGFR-2 messengers were increased by hypoxia ($^{*}P < 0.05$ and $^{**}P < 0.01$ versus the respective normoxic; ANOVA). The increase in VEGF mRNA (**B**) was lower in sst_1-KO than in WT retinas ($\S P < 0.05$ versus hypoxic WT; ANOVA). Data were analyzed by the formula $2^{-\Delta\Delta CT}$ using *Rpl13a* as internal standard. Each column represents the mean ± SE of data from four samples. Each sample refers to the mRNA extracted from three retinas.

tum, CYN administration using in vivo microdialysis blocks the SRIF-induced stimulation of dopamine.[39] The results of the present work are the first demonstration of the sst_2 antagonistic properties of CYN in an OIR model. In our work, CYN concentrations affecting both retinal neovascularization and the VEGF system are in line with those used in previous work. Indeed, the intravenous administration of CYN doses ranging from 1.0 to 3.0 mg kg^{-1} blocks the octreotide-evoked inhibition of baseline discharge of mesenteric afferent nerves of the jejunum in the rat.[24] In addition, the microinjection in the rat dorsal vagal complex of 0.1 nanomoles CYN (~0.5 μg kg^{-1})

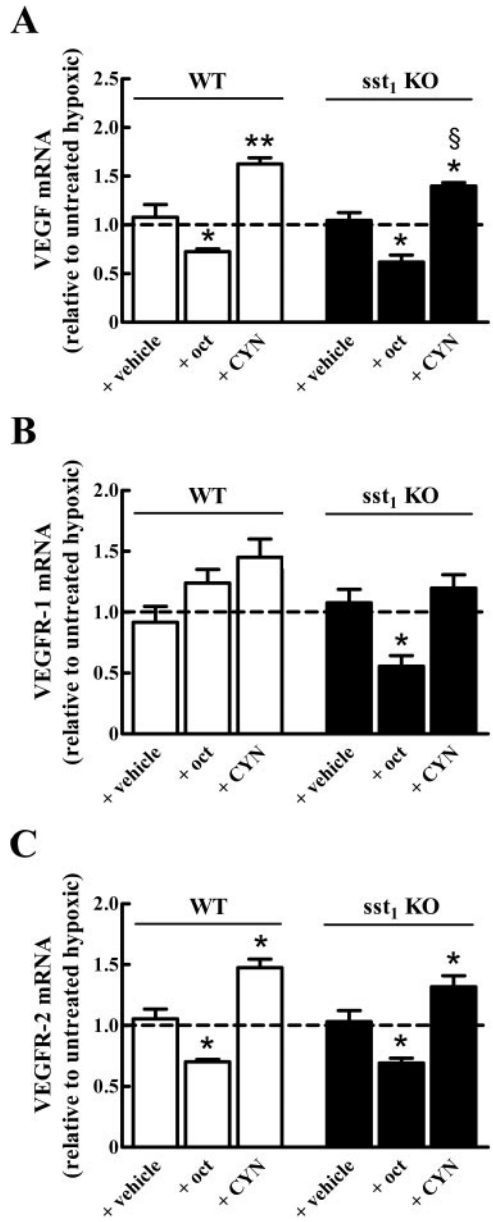

FIGURE 3. QPCR evaluation of VEGF (**A**), VEGFR-1 (**B**) and VEGFR-2 (**C**) in hypoxic WT (□) and sst_1-KO (■) retinas after treatment with vehicle, 0.02 mg kg^{-1} octreotide or 0.5 mg kg^{-1} CYN. (**A**) Octreotide decreased VEGF levels in both WT and sst_1-KO retinas ($^{*}P < 0.05$ versus the respective untreated retinas; ANOVA), whereas CYN increased VEGF mRNA ($^{*}P < 0.05$ and $^{**}P < 0.01$ versus the respective untreated retinas; ANOVA). The CYN-induced increase was lower in sst_1-KO than in WT retinas ($\S P < 0.05$ versus CYN-treated WT; ANOVA). (**B**) Octreotide did not affect VEGFR-1 mRNA in WT retinas, whereas it decreased VEGFR-1 mRNA in sst_1-KO retinas ($^{*}P < 0.05$ versus the respective untreated retinas; ANOVA). CYN did not influence VEGFR-1 mRNA neither in WT nor in sst_1-KO. (**C**) VEGFR-2 mRNA was decreased by octreotide, whereas it was increased by CYN in both WT and sst_1-KO retinas ($^{*}P < 0.05$ versus the respective untreated retinas; ANOVA). Data were analyzed by the formula $2^{-\Delta\Delta CT}$ using *Rpl13a* as internal standard. Each column represents the mean ± SE of data from four samples. Each sample refers to the mRNA extracted from three retinas. oct, octreotide.

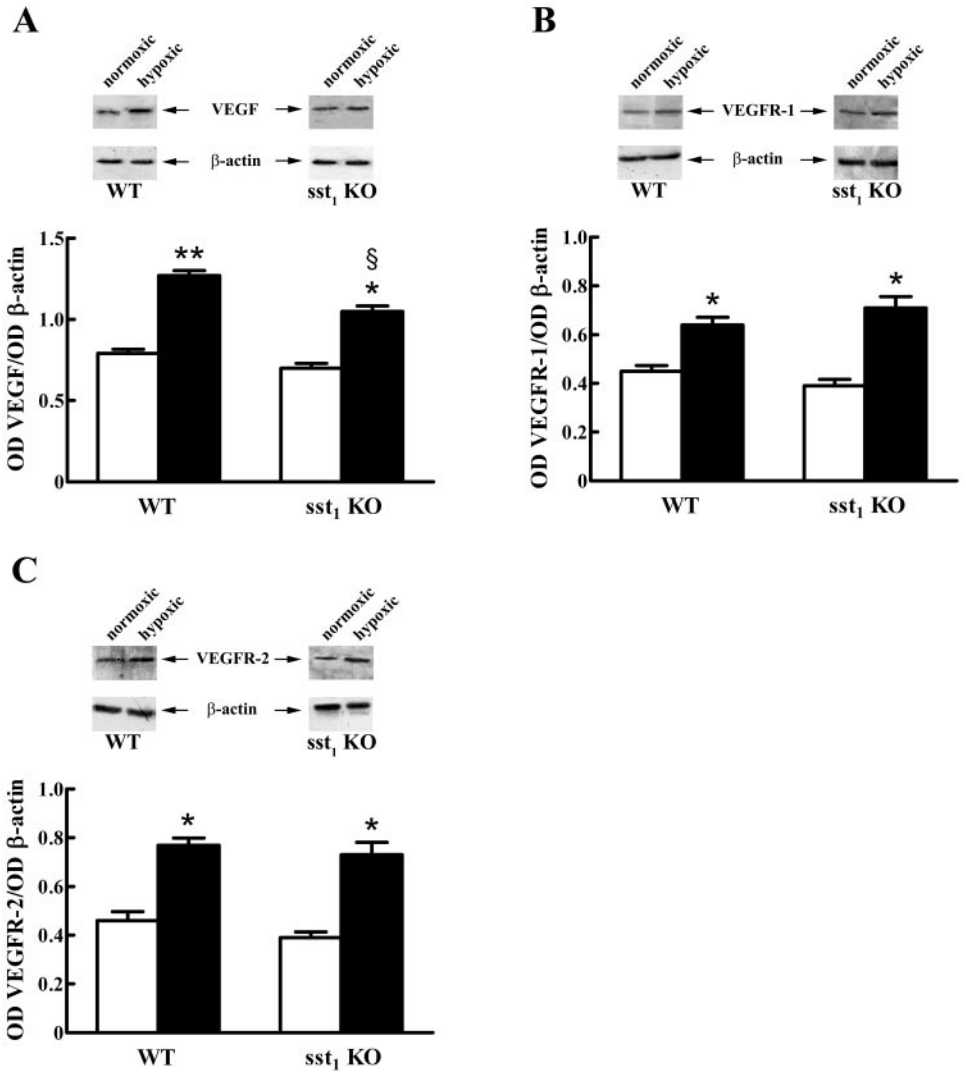

FIGURE 4. Levels of VEGF (**A**), VEGFR-1 (**B**), and VEGFR-2 (**C**) in normoxic (□) and hypoxic (■) conditions, as evaluated by Western blot using β-actin as a loading control in WT and sst_1-KO retinas. (**A–C**) Densitometric analysis showed that VEGF, VEGFR-1, and VEGFR-2 were increased by hypoxia ($^*P < 0.05$ and $^{**}P < 0.01$ versus the respective normoxic; ANOVA). The VEGF increase (**A**) was lower in sst_1-KO than in WT retinas ($\S P < 0.05$ versus hypoxic WT; ANOVA). Each column represents the mean ± SE of data from three samples. Each sample refers to the protein extracted from five retinas.

prevents the SRIF-induced inhibition of pancreatic secretion.[20] Moreover, another sst_2 antagonist, BIM-23627, dose dependently decreases growth hormone secretion in dexamethasone-treated rats, with minimum effects at 0.02 mg kg^{-1} and maximum effects at 2.0 mg kg^{-1}.[23] In another study, BIM-23627 at 0.5 mg kg^{-1} has been found to improve the catabolic effects of dexamethasone on different parameters, including growth, epididymal fat accumulation, glucose homeostasis, and insulin activity.[21] In addition, the intracerebroventricular application of 2.5 nanomoles BIM-23627 (~0.01 mg kg^{-1}) blocks sst_{2A} internalization in a rat model of middle cerebral artery occlusion.[22] In our OIR model, there were findings in favor of the specificity of CYN. Indeed, the lack of CYN′s effects on retinal neovascularization in sst_2-KO mice confirmed the specific action of CYN at sst_2. In addition, the dose dependency of CYN′s effects on the VEGF levels in sst_1-KO retinas (described in the next section) indicated that the CYN concentration required to activate overexpressed sst_2 was four times higher than in WT retinas.

Effects of SRIF Analogues on Neovascularization

In agreement with previous results,[12] the neovascularization response to hypoxic insult is significantly worsened by the lack of sst_2, whereas a chronic overexpression of sst_2 (as in sst_1-KO retinas) does not attenuate retinal neovascularization. In agreement with previous findings,[9–11] this study describes ameliorative effects of octreotide on retinal neovascularization in the OIR model. Recently, nonpeptide SRIF receptor agonists specifically targeting sst_2 have been found to inhibit retinal neovascularization in the OIR model.[9] Our additional result that blocking of sst_2 results in a worsened angiogenic response to hypoxic insult is in line with the finding that retinal neovascularization increases in sst_2-KO mice[12] and suggests a constitutive activity of the receptor in hypoxic conditions. In line with this possibility, a constitutive activity of sst_2 in ischemic conditions has been recently demonstrated in an in vitro model of the ischemic mouse retina.[40] In this respect, a recombinant truncated form of the rat sst_2 has been shown to display agonist-independent, constitutive activity,[41] and constitutive activation of sst_2 has been demonstrated in mouse pituitary corticotroph cells.[42]

Effects of SRIF Analogues on the VEGF System

Both experimental and clinical studies have reported an important role of VEGF in pathologic retinal angiogenesis.[43] However, the sites of VEGF release and those of VEGF actions in the retina are poorly understood. Of the VEGF receptors, VEGFR-2 is considered to be the receptor that mediates functional VEGF signaling in endothelial cells, whereas the function of VEGFR-1 and the possibility that VEGFR-1 affects endothelial cells re-

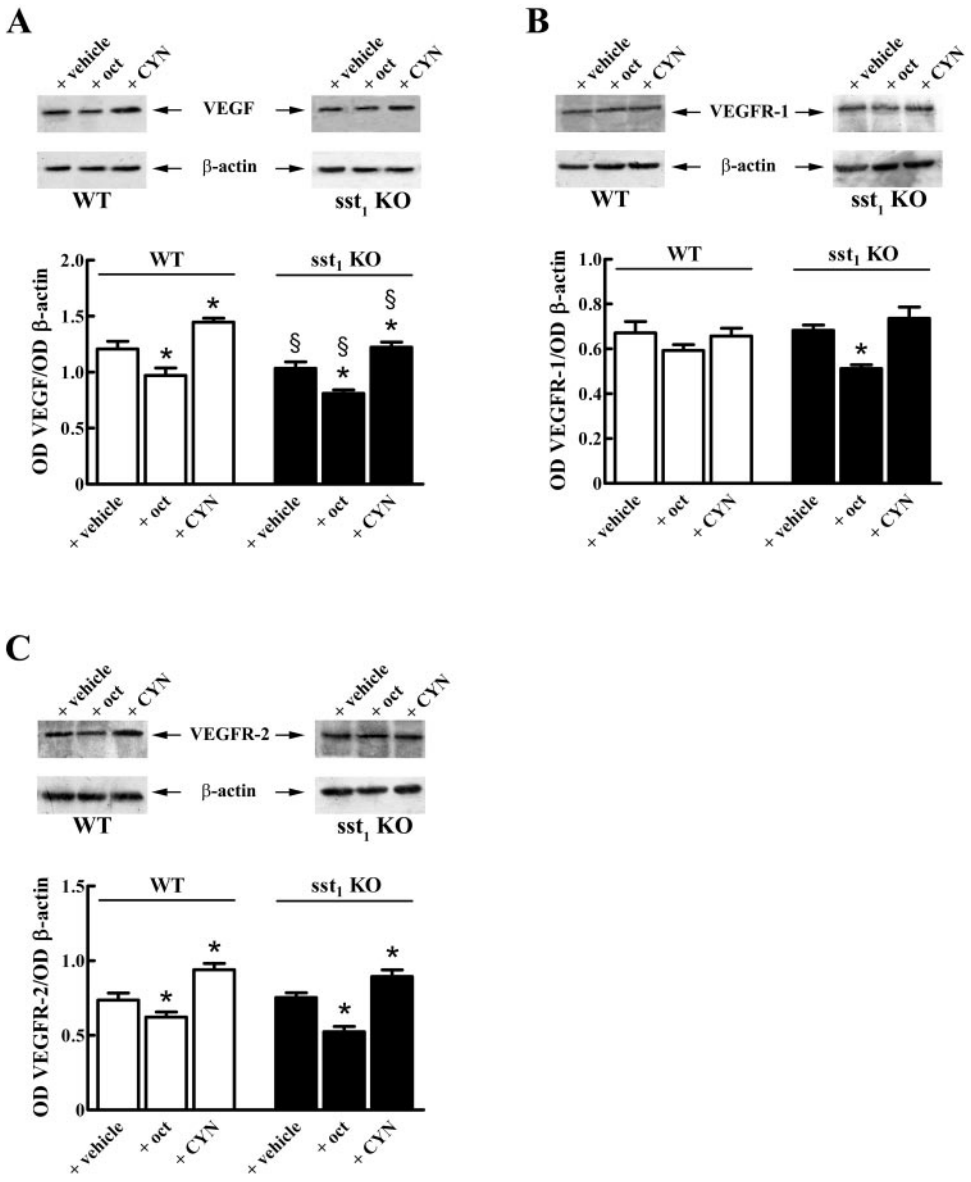

FIGURE 5. Levels of VEGF (**A**), VEGFR-1 (**B**), and VEGFR-2 (**C**) in hypoxic WT (□) and sst_1-KO (■) retinas after treatment with vehicle, 0.02 mg kg^{-1} octreotide or 0.5 mg kg^{-1} CYN, as evaluated by Western blot using β-actin as a loading control. (**A**) VEGF level in vehicle-treated sst_1-KO was significantly lower than in WT (§$P < 0.05$ versus vehicle-treated WT; ANOVA). In both WT and sst_1-KO retinas, octreotide decreased VEGF which was, in contrast, increased by CYN (*$P < 0.05$ versus the respective vehicle-treated retinas; ANOVA). Compared with WT, in sst_1-KO retinas, the VEGF decrease after octreotide was higher, whereas the increase in VEGF after CYN was lower (§$P < 0.05$ versus octreotide- or CYN-treated WT retinas; ANOVA). (**B**) Octreotide did not affect VEGFR-1 in WT retinas, whereas it decreased VEGFR-1 levels in sst_1-KO retinas (*$P < 0.05$ versus the respective untreated retinas; ANOVA). CYN did not influence VEGFR-1 in WT or in sst_1-KO retinas. (**C**) VEGFR-2 was decreased by octreotide, whereas it was increased by CYN in both WT and sst_1-KO retinas (*$P < 0.05$ versus the respective untreated retinas; ANOVA). Each column represents the mean ± SE of data from three samples. Each sample refers to the protein extracted from five retinas. oct, octreotide.

main to be fully disclosed.[44] Our finding that hypoxia increases the levels of VEGF and its receptors is consistent with previous findings.[12,45–48] Our additional finding that SRIF analogues influence VEGF production is in agreement with previous results from in vitro studies. In human glioma cells, for instance, SRIF or the sst_2-selective agonists octreotide and L-054522 potently inhibit basal VEGF production with less effect on hypoxia-induced VEGF release.[49] In human retinal pigment epithelial cells, SRIF reduces VEGF mRNA through sst_2.[50] In pituitary tumor cells, SRIF influences VEGF secretion differently, depending on the spectrum of expressed SRIF receptor subtypes, including sst_2.[51] A few results are available in in vivo models of proliferating endothelium. A recent study, in particular, demonstrates that octreotide markedly decreases splanchnic neovascularization and VEGF expression in portal hypertensive rats.[6] In addition, octreotide ameliorates histomorphologic changes, including vessel dilatation and VEGF increase associated with portal hypertensive enteropathy in rats.[5] Our recent results in the mouse retina demonstrate that enhanced somatostatinergic function at sst_2, as in sst_1-KO mice, limits the hypoxia-induced VEGF increase whereas sst_2 loss upregulates this increase,[12] thus suggesting a role for sst_2 in the regulation of VEGF homeostasis. In this study, we provided the first demonstration that sst_2 is coupled to a modulation of the VEGF system in an in vivo model of retinal neovascularization. Indeed, the hypoxia-induced increase in VEGF and VEGFR-2 was consistently reduced by octreotide whereas it was drastically increased by sst_2 blockade with CYN. In particular, the fact that VEGFR-2, but not VEGFR-1, was influenced by SRIF analogues is in line with the finding that VEGFR-2 is the receptor principally involved in retinal angiogenesis and suggests that it may act downstream of the sst_2-induced modulation of retinal neovascularization. In this respect, the finding that in hypoxic retinas, octreotide downregulates VEGF and VEGFR-2 is particularly intriguing in light of a possible therapeutic use of sst_2 agonists to counteract retinal neovascularization by influencing the VEGF system. The hypoxic level of VEGF after octreotide treatment was lower in sst_1-KO than in WT mice, indicating that in WT, sst_2 may be saturated by 0.02 mg kg^{-1} octreotide. In sst_1-KO retinas, we also observed a dose dependency of CYN's effects on VEGF levels, thus confirming a specific action of CYN at sst_2 and suggesting that overexpressed sst_2 is not saturated by CYN at doses below 2.0 mg kg^{-1}. The finding that hypoxic levels of VEGFR-1 are downregulated by octreotide in sst_1-KO but not in WT mice is in line with previous results demonstrating that the

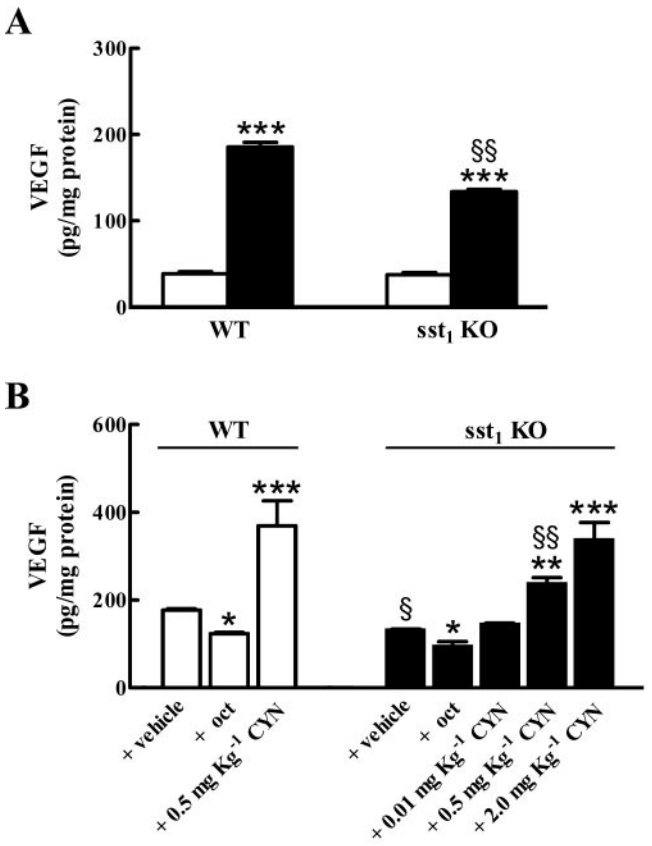

FIGURE 6. VEGF protein levels in WT and sst_1-KO retinas, as quantified with ELISA. (**A**) VEGF levels in normoxic (□) and hypoxic (■) conditions. In both WT and sst_1-KO, normoxic VEGF was increased by hypoxia (***$P < 0.001$ versus the respective normoxic; ANOVA). The VEGF increase was lower in sst_1-KO than in WT retinas (§§$P < 0.01$ versus hypoxic WT; ANOVA). (**B**) VEGF levels in hypoxic WT (□) and sst_1-KO (■) retinas after treatment with vehicle or SRIF analogues. VEGF level in vehicle-treated sst_1-KO was significantly lower than in WT (§$P < 0.05$ versus vehicle-treated WT; ANOVA). In both WT and sst_1-KO, octreotide was used at 0.02 mg kg^{-1}. In WT, CYN was used at 0.5 mg kg^{-1}, whereas increasing concentrations were used in sst_1-KO. In both WT and sst_1-KO retinas, octreotide decreased VEGF (*$P < 0.05$ versus respective vehicle-treated retinas; ANOVA). In sst_1-KO retinas, the VEGF decrease after octreotide was higher than in WT (§$P < 0.05$ versus octreotide-treated WT; ANOVA). WT mice treated with CYN showed a significant increase in retinal levels of VEGF (***$P < 0.001$ versus vehicle-treated WT; ANOVA). In sst_1-KO retinas, a dose-dependent increase of VEGF was observed after treatment with increasing concentrations of CYN, with no effects at 0.01 mg kg^{-1}; an increase at 0.5 mg kg^{-1} (**$P < 0.01$ versus vehicle-treated sst_1-KO; ANOVA), but a significantly lower than in WT (§§$P < 0.01$ vs. 0.5 mg kg^{-1} CYN-treated WT; ANOVA); and maximum at 2.0 mg kg^{-1} (***$P < 0.001$ versus vehicle-treated sst_1-KO; ANOVA). Each column represents the mean ± SE of data from three samples. Each sample refers to the protein extracted from two retinas. oct, octreotide.

density of retinal sst_2 represents the rate-limiting factor for sst_2-mediated effects.[37]

Receptor-Mediated Effects of SRIF Analogues

Despite the growing evidence that sst_2 agonists may exert angioinhibitory activity, the exact role of receptor-mediated effects in the retina is still unknown. The simplest explanation is that in our model SRIF analogues act on sst_2 expressed by endothelial cells of retinal blood vessels. However, sst_2 does not seem to be expressed by retinal endothelial cells in rodents, although there is evidence that sst_2 is localized to numerous cells in the neuroretina.[52] One possibility is that quiescent vascular endothelial cells do not express sst_2 and that this receptor is expressed when the endothelial cells begin to grow. In this respect, it has been reported that, in cultured human veins, proliferating angiogenic sprouts of vascular endothelium express sst_2.[53] In addition, immunostaining for sst_2 can be detected in proliferating but not quiescent human umbilical vein endothelial cells.[54] Moreover, in human eyes with late stages of age-related maculopathy and characterized by choroidal neovascularization, newly formed endothelial cells strongly express sst_2.[55] Finally, the pattern of sst_2 expression in patients with diabetic retinopathy indicates that beneficial effects of sst_2 agonists may depend on the presence of sst_2 on newly formed vessels.[56] Recently, a relationship between sst_2 levels and octreotide efficacy to inhibit angiogenesis has been demonstrated in rats with advanced stages of portal hypertension.[6] The issue of dynamic changes in sst_2 expression in mouse models of hypoxia-induced growing vascular endothelium remains to be addressed.

Clinical Implication

Most of the therapeutic interventions against diabetic retinopathy have focused on the mechanisms and the factors leading to new vessel growth. In this respect, based on experimental evidence, there has been great interest in the development of anti-VEGF compounds for the treatment of proliferative diabetic retinopathy, such as antibodies, antisense oligonucleotides, and small interfering RNAs that target VEGF. However, anti-VEGF therapy shows a loss of efficacy as the neovasculature develops. Moreover, the therapy stabilizes the disease rather than improving vision, and the regression of neovascularization is rarely permanent.[57] On the other hand, several limited clinical trials using the SRIF analogue octreotide in the treatment of retinopathy has been performed giving mixed results about the efficacy of the treatment (for a review, see Ref. 8). For instance, in a small-scale randomized controlled study of 23 patients with severe nonproliferative diabetic retinopathy or early proliferative diabetic retinopathy, octreotide has been found to reduce the requirement for laser photocoagulation compared with conventional treatment. However, the two large-scale, muticenter, randomized placebo-controlled clinical trials initiated by Novartis (Basel, Switzerland), have been inconclusive on the effect of octreotide on the progression of retinopathy, but have shown some benefit on visual acuity.[3] Our finding that in hypoxic retinas, octreotide downregulates VEGF and VEGFR-2 is particularly intriguing in light of a possible therapeutic use of sst_2 agonists to counteract retinal neovascularization by influencing the VEGF system and strongly supports the validity of combination drug therapy for vasoproliferative disorders in the retina.

CONCLUSIONS

SRIF analogues may interfere with the retinopathy-producing cascade at different levels, including proangiogenic factors. We have demonstrated that SRIF analogues with high specificity for sst_2 regulate retinal angiogenesis and that their effects involve a modulation of the VEGF system. Thus, the effectiveness of SRIF analogues in diabetic retinopathy could be due to local growth factor–lowering effects, although direct antiangiogenic effects of these compounds cannot be excluded.

Acknowledgments

The authors thank Angelo Gazzano and Gino Bertolini (University of Pisa, Italy) for assistance with the mouse colonies.

References

1. Hoyer D, Bell GI, Berelowitz M, et al. Classification and nomenclature of somatostatin receptors. *Trends Pharmacol Sci.* 1995;16:86–88.
2. Cervia D, Casini G, Bagnoli P. Physiology and pathology of somatostatin in the mammalian retina: a current view. *Mol Cell Endocrinol.* 2008;286:112–122.
3. Boehm BO. Use of long-acting somatostatin analogue treatment in diabetic retinopathy. *Dev Ophthalmol.* 2007;39:111–121.
4. Dasgupta P. Somatostatin analogues: multiple roles in cellular proliferation, neoplasia, and angiogenesis. *Pharmacol Ther.* 2004;102:61–85.
5. Aydede H, Seda Vatansever H, Erhan Y, Ilkgül O. Effects of ocreotide on intestinal mucosa in rats with portal hypertensive enteropathy. *Acta Histochem.* 2009;111:74–82.
6. Mejias M, Garcia-Pras E, Tiani C, Bosch J, Fernandez M. The somatostatin analogue octreotide inhibits angiogenesis in the earliest, but not in advanced, stages of portal hypertension in rats. *J Cell Mol Med.* 2008;12:1690–1699.
7. Palii SS, Caballero S Jr., Shapiro G, Grant MB. Medical treatment of diabetic retinopathy with somatostatin analogues. *Expert Opin Investig Drugs.* 2007;16:73–82.
8. Grant MB, Caballero S Jr. The potential role of octreotide in the treatment of diabetic retinopathy. *Treat Endocrinol.* 2005;4:199–203.
9. Palii SS, Afzal A, Shaw LC, et al. Nonpeptide somatostatin receptor agonists specifically target ocular neovascularization via the somatostatin type 2 receptor. *Invest Ophthalmol Vis Sci.* 2008;49:5094–5102.
10. Wilkinson-Berka JL, Lofthouse S, Jaworski K, Ninkovic S, Tachas G, Wraight CJ. An antisense oligonucleotide targeting the growth hormone receptor inhibits neovascularization in a mouse model of retinopathy. *Mol Vis.* 2007;13:1529–1538.
11. Higgins MD, Yan Y, Schrier BK. Somatostatin analogs inhibit neonatal retinal neovascularization. *Exp Eye Res.* 2002;74:553–559.
12. Dal Monte M, Cammalleri M, Martini D, Casini G, Bagnoli P. Antiangiogenic role of somatostatin receptor 2 in a model of hypoxia-induced neovascularization in the retina: results from transgenic mice. *Invest Ophtalmol Vis Sci.* 2007;48:3480–3489.
13. Casini G, Dal Monte M, Petrucci C, et al. Altered morphology of rod bipolar cell axonal terminals in the retinas of mice carrying genetic deletion of somatostatin subtype receptor 1 or 2. *Eur J Neurosci.* 2004;19:43–54.
14. Dal Monte M, Petrucci C, Vasilaki A, et al. Genetic deletion of somatostatin receptor 1 alters somatostatinergic transmission in the mouse retina. *Neuropharmacology.* 2003;45:1080–1092.
15. Allen JP, Hathway GJ, Clarke NJ, et al. Somatostatin receptor 2 knockout/lacZ knockin mice show impaired motor coordination and reveal sites of somatostatin action within the striatum. *Eur J Neurosci.* 2003;17:1881–1895.
16. Kreienkamp HJ, Akgun E, Baumeister H, Meyerhof W, Richter D. Somatostatin receptor subtype 1 modulates basal inhibition of growth hormone release in somatotrophs. *FEBS Lett.* 1999;462:464–466.
17. Smith LEH, Wesolowski E, McLellan A, et al. Oxygen-induced retinopathy in the mouse. *Invest Ophthalmol Vis Sci.* 1994;35:101–111.
18. Nunn C, Schoeffer P, Langenegger D, Hoyer D. Functional characterisation of the putative somatostatin sst2 receptor antagonist CYN 154806. *Naunyn Schmiedebergs Arch Pharmacol.* 2003;367:1–9.
19. Weckbecker G, Lewis I, Albert R, Schmid HA, Hoyer D, Bruns C. Opportunities in somatostatin research: biological, chemical and therapeutic aspects. *Nat Rev Drug Discov.* 2003;2:999–1017.
20. Liao Z, Li ZS, Lu Y, Wang WZ. Microinjection of exogenous somatostatin in the dorsal vagal complex inhibits pancreatic secretion via somatostatin receptor-2 in rats. *Am J Physiol Gastrointest Liver Physiol.* 2007;292:G746–G752.
21. Tulipano G, Rossi E, Culler MD, et al. The somatostatin subtype-2 receptor antagonist, BIM-23627, improves the catabolic effects induced by long-term glucocorticoid treatment in the rat. *Regul Pept.* 2005;125:85–92.
22. Stumm RK, Zhou C, Schulz S, et al. Somatostatin receptor 2 is activated in cortical neurons and contributes to neurodegeneration after focal ischemia. *J Neurosci.* 2004;24:11404–11415.
23. Tulipano G, Soldi D, Bagnasco M, et al. Characterization of new selective somatostatin receptor subtype-2 (sst2) antagonists, BIM-23627 and BIM-23454 effects of BIM-23627 on GH release in anesthetized male rats after short-term high-dose dexamethasone treatment. *Endocrinology.* 2002;143:1218–1224.
24. Booth CE, Kirkup AJ, Hicks GA, Humphrey PP, Grundy D. Somatostatin sst(2) receptor-mediated inhibition of mesenteric afferent nerves of the jejunum in the anesthetized rat. *Gastroenterology.* 2001;121:358–369.
25. D'Amato R, Wesolowski E, Smith LE. Microscopic visualization of the retina by angiography with high-molecular-weight fluorescein-labeled dextrans in the mouse. *Microvasc Res.* 1993;46:135–142.
26. Rozen S, Skaletsky H. Primer3 on the WWW for general users and for biologist programmers. *Methods Mol Biol.* 2000;132:365–386.
27. Wang X, Seed B. A PCR primer bank for quantitative gene expression analysis. *Nucleic Acids Res.* 2003;31:e154.
28. Pattyn F, Speleman F, De Paepe A, Vandesompele J. RTPrimerDB: the real-time PCR primer and probe database. *Nucleic Acids Res.* 2003;31:122–123.
29. Livak KJ, Schmittgen TD. Analysis of relative gene expression data using real-time quantitative PCR and the 2(−Delta Delta C(T)) Method. *Methods.* 2001;25:402–408.
30. Bradford MM. A rapid and sensitive method for the quantitation of microgram quantities of protein utilizing the principle of protein-dye binding. *Anal Biochem.* 1976;72:248–254.
31. Laemmli UK. Cleavage of structural proteins during the assembly of the head of bacteriophage T4. *Nature.* 1970;227:680–685.
32. Nagai N, Izumi-Nagai K, Oike Y, et al. Suppression of diabetes-induced retinal inflammation by blocking the angiotensin II type 1 receptor or its downstream nuclear factor-κB pathway. *Invest Ophthalmol Vis Sci.* 2007;48:4342–4350.
33. Obrosova IG, Drel VR, Kumagai AK, Szabo C, Pacher P, Stevens MJ. Early diabetes-induced biochemical changes in the retina: comparison of rat and mouse models. *Diabetologia.* 2006;49:2525–2533.
34. Dejneka NS, Kuroki AM, Fosnot J, Tang W, Tolentino MJ, Bennett J. Systemic rapamycin inhibits retinal and choroidal neovascularization in mice. *Mol Vis.* 2004;10:964–972.
35. Elner SG, Elner VM, Yoshida A, Dick RD, Brewer GJ. Effects of tetrathiomolybdate in a mouse model of retinal neovascularization. *Invest Ophthalmol Vis Sci.* 2005;46:299–303.
36. Cervia D, Nunn C, Bagnoli P. Multiple signalling transduction mechanisms differentially coupled to somatostatin receptor subtypes: a current view. *Curr Enz Inhib.* 2005;1:265–279.
37. Pavan B, Fiorini S, Dal Monte M, et al. Somatostatin coupling to adenylyl cyclase activity in the mouse retina. *Naunyn-Schmiedeberg's Arch Pharmacol.* 2004;370:91–98.
38. Stragier B, Clinckers R, Meurs A, et al. Involvement of the somatostatin-2 receptor in the anti-convulsant effect of angiotensin IV against pilocarpine-induced limbic seizures in rats. *J Neurochem.* 2006;98:1100–1113.
39. Hathway GJ, Humphrey PP, Kendrick KM. Evidence that somatostatin sst2 receptors mediate striatal dopamine release. *Br J Pharmacol.* 1999;128:1346–1352.
40. Cervia D, Martini D, Ristori C, et al. Modulation of the neuronal response to ischaemia by somatostatin analogues in wild-type and knock-out mouse retinas. *J Neurochem.* 2008;106:2224–2235.
41. Schwartkop CP, Kreienkamp HJ, Richter D. Agonist-independent internalization and activity of a C-terminally truncated somatostatin receptor subtype 2 (delta349). *J Neurochem.* 1999;72:1275–1282.
42. Ben-Shlomo A, Pichurin O, Barshop NJ, et al. Selective regulation of somatostatin receptor subtype signaling: evidence for constitutive receptor activation. *Mol Endocrinol.* 2007;21:2565–2578.
43. Kvanta A. Ocular angiogenesis: the role of growth factors. *Acta Ophthalmol Scand.* 2006;84:282–288.
44. Witmer AN, Vrensen GF, Van Noorden CJ, Schlingemann RO. Vascular endothelial growth factors and angiogenesis in eye disease. *Prog Retin Eye Res.* 2003;22:1–29.

45. Goldenberg-Cohen N, Dadon S, Avraham BC et al. Molecular and histological changes following central retinal artery occlusion in a mouse model. *Exp Eye Res.* 2008;87:327–333.
46. Kaur C, Sivakamur V, Foulds WS. Early response of neurons and glial cells to hypoxia in the retina. *Invest Ophthalmol Vis Sci.* 2006;47:1126–1141.
47. Werdich XQ, McCollum GW, Rajaratnam VS, Penn JS. Variable oxygen and retinal VEGF levels : correlation with incidence and severity of pathology in a rat model of oxygen-induced retinopathy. *Exp Eye Res.* 2004;79:623–630.
48. McLeod DS, Taomoto M, Cao J, Zhu Z, Witte L, Lutty GA. Localization of the VEGF receptor-2 (KDR/Flk-1) and effects of blocking it in oxygen-induced retinopathy. *Invest Ophthalmol Vis Sci.* 2002;43:474–482.
49. Mentlein R, Eichler O, Forstreuter F, Held-Feindt J. Somatostatin inhibits the production of vascular endothelial growth factor in human glioma cells. *Int J Cancer.* 2001;92:545–550.
50. Sall JW, Klisovic DD, O'Dorisio MS, Katz SE. Somatostatin inhibits IGF-1 mediated induction of VEGF in human retinal pigment epithelial cells. *Exp Eye Res.* 2004;79:465–476.
51. Lawnicka H, Pisarek H, Kunert-Radek J, Pawlikowski M. Effects of somatostatin on vascular endothelial growth factor (VEGF) secretion from non-functioning pituitary tumoral cells incubated in vitro. *Neuro Endocrinol Lett.* 2008;29:113–116.
52. Casini G, Catalani E, Dal Monte M, Bagnoli P. Functional aspects of the somatostatinergic system in the retina and the potential therapeutic role of somatostatin in retina disease. *Histol Histopathol.* 2005;20:615–632.
53. Watson JC, Balster DA, Gebhardt BM, et al. Growing vascular endothelial cells express somatostatin subtype 2 receptors. *Br J Cancer.* 2001;85:266–272.
54. Adams RL, Adams IP, Lindow SW, Zhong W, Atkin SL. Somatostatin receptors 2 and 5 are preferentially expressed in proliferating endothelium. *Br J Cancer.* 2005;92:1493–1498.
55. Lambooij AC, Kuijpers RW, van Lichtenauer-Kaligis EG, et al. Somatostatin receptor 2A expression in choroidal neovascularization secondary to age-related macular degeneration. *Invest Ophthalmol Vis Sci.* 2000;41:2329–2335.
56. van Hagen PM, Baarsma GS, Mooy CM, et al. Somatostatin and somatostatin receptors in retinal diseases. *Eur J Endocrinol.* 2000; 143(suppl 1):S43–S51.
57. Bradley J, Ju M, Robinson GS. Combination therapy for the treatment of ocular neovascularization. *Angiogenesis.* 2007;10:141–148.